Superpositions in Atomic Quantum Rings

R. Kanamoto[1], P. Öhberg[2], and E. M. Wright[3]

[1] Department of Physics, Meiji University, Kawasaki, Kanagawa 214-8571, Japan
[2] SUPA, Institute of Photonics and Quantum Sciences, Heriot Watt University, Edinburgh EH14 4AS, UK
[3] College of Optical Sciences, University of Arizona, Tucson AZ 85721, USA

Abstract. An atomic quantum ring involves ultracold atoms that are trapped circumferentially on a ring that is pierced at its center by a flux tube arising from the light-induced gauge potential due to applied Laguerre-Gaussian fields. In this paper we show that by using optical coherent state superpositions to produce the light-induced gauge potentials we can create the situation in which the trapped atoms are simultaneously exposed to two distinct flux tubes thereby creating superpositions in atomic quantum rings. We consider the examples of both a ring geometry and harmonic trapping, and in both cases we show that the ground state of the quantum system is a superposition of counter-rotating states of the atom trapped on the two distinct flux tubes.

1. Introduction

The theoretical concept of creating artificial gauge potentials for neutral atoms using spatially tailored light fields has now reached maturity, see Ref. [1] for a comprehensive theoretical review, and the recent experiments in which an artificial magnetic field was created in a Rubidium Bose-Einstein condensate [2], which has most notably led to creation of quantized vortices [3], spin-orbit coupling [4] and strong effective magnetic fields in optical lattices [5]. Being able to create artificial gauge fields, both abelian and non-abelian [6, 7], has opened up new avenues of research such as creating exotic matter wave states [8], quantized vortices being a simple example [3], gauge potentials in optical lattices allowing for the study of the Harper equation and Hofstadter butterfly [9], the creation of Aharanov-Bohm like effects in atomic gases [10], and the exploration of analogies and differences with condensed matter and particle physics ideas [11, 12, 13]. Of particular interest for this paper is the fact that using Laguerre-Gaussian laser fields, that carry orbital angular momentum, in interaction with a three-level atom, can yield an induced gauge potential that acts as an effective flux tube [14]. This is significant in that if the atom is trapped in a radially symmetric potential and the flux tube pierces the potential, then varying the flux can vary the angular momentum properties of the ground state trapped atom [15, 16, 17].

The goal of the present paper is to initiate a new line of research involving artificial gauge potentials formed using quantum mechanical applied light fields, in particular optical coherent state superpositions [18, 19]. The concept is that if the quantum nature of the applied light can be transferred to the matter waves then we open up the possibility of exposing the atom simultaneously to a superposition of two or more artificial gauge potentials. To introduce and explore this possibility we consider the example of an atomic quantum ring, both idealized and in a harmonic trap. An atomic quantum ring involves ultracold atoms that are trapped circumferentially on a ring that is pierced at its center by a flux tube arising from the light-induced gauge potential due to applied Laguerre-Gaussian fields [16, 17]. With a finite flux piercing the ring the ground state corresponds to a rotating state. Here we show that by using optical coherent state superpositions to produce the light-induced gauge potentials we can create the situation in which the trapped atoms are simultaneously exposed to two distinct flux tubes thereby creating superpositions in atomic quantum rings. In particular, we show that the ground state is a quantum superposition of counter-rotating atomic states.

In section 2 we overview the basic formulation of the field-induced gauge potential for a singe atom in the electromagnetically induced transparency (EIT) configuration [1, 14]. An effective Hamiltonian for the dark-state atom and its eigensolutions are given for the harmonic and ring potentials. Section 3 extends the standard dark-state scheme to the case of a nonclassical control field. We show that the superposition of distinct motional states has a lower energy than the statistical mixture of those states.

2. Atomic quantum ring

For the sake of clarity in presentation, and to solidify notation, in this section we review the basic physical ideas underpinning the atomic quantum ring for classical applied fields as described by coherent states. First we set up the model equations as described in Ref. [14], and then we turn to dark states and the effective gauge potential and flux tube. Finally we discuss the quantum motional eigenstates for the cases of a ring geometry and harmonic trapping.

2.1. Model equations

In a series of recent papers it has been shown how carefully shaped light beams which are incident on cold atoms can be used for creating strong gauge potentials in a cloud of neutral atoms. This effect relies on the interplay between two laser beams and a Λ-type level structure of the atoms, as shown in Fig. 1. In the following we consider a single atom which is characterized by two hyperfine ground levels $|1\rangle$ and $|2\rangle$ of equal energies $\hbar\omega_1 = \hbar\omega_2$, and an electronic excited level $|3\rangle$ with energy $\hbar\omega_3$. The atom interacts with two laser beams. The first beam which we refer to as the probe beam, is coupled with the transition $|1\rangle \leftrightarrow |3\rangle$, whereas the second beam, the control beam, drives the transition $|2\rangle \leftrightarrow |3\rangle$. The probe field is characterized by a wave vector $\boldsymbol{k}_p$, and a central frequency $\omega_p = ck_p$. The control laser, on the other hand, has a wave vector $\boldsymbol{k}_c$ and a frequency ω_c. We use Laguerre-Gaussian (LG) beams for the probe and control fields, with the lowest radial quantum number and distinct orbital angular momenta per photon $\hbar\ell_c$ for the control field, and $\hbar\ell_p$ for the probe field, respectively. Henceforth we choose the control and probe fields to have equal frequency $\omega_p = \omega_c = \omega$, equal magnitude of winding numbers of opposite sign $\ell_c = -\ell_p = \ell$, and take $\boldsymbol{k}_c$ and $\boldsymbol{k}_p$ collinear along the z axis.

The Hamiltonian for the electronic degree of freedom of an atom interacting with quantized light fields in the rotating-wave approximation is given by

$$\hat{h}(\boldsymbol{r}) = \epsilon_{31}|3\rangle\langle 3| - \hbar\chi(\boldsymbol{r})\left(\hat{a}_p e^{-i\ell\phi}|3\rangle\langle 1| + \hat{a}_c e^{i\ell\phi}|3\rangle\langle 2| + h.c.\right) \tag{1}$$

where $\epsilon_{31} = \hbar(\omega_3 - \omega_1 - \omega)$ is the energy of the detuning from single-photon resonance, with $\hbar\omega_j$ being the electronic energy of the atomic level $j = 1, 2, 3$. Here the Rabi frequency per photon coupling the ground and excited states is denoted as $\chi(\boldsymbol{r})$, and $\hat{a}_p$, $\hat{a}_c$ are the annihilation operators of a photon in the probe and control fields. In deriving the above Hamiltonian for the electronic degree of freedom we have assumed that the atomic motion is restricted to the two dimension plane $\boldsymbol{r} = (r, \phi)$ with $r = \sqrt{x^2 + y^2}$, due to a tight confinement along z direction. The spatial dependence of the Hamiltonian then comes from the space-dependent coupling associated with the LG beams.

In this subsection we suppose that the control, and probe fields may be described by coherent states $|\alpha\rangle$, and $|\beta\rangle$, respectively. The field state is then expressed by $|\Psi_f\rangle = |\alpha\rangle_c|\beta\rangle_p$ and the effective Hamiltonian for an atom $\hat{h}_a(\boldsymbol{r}) \equiv \langle\Psi_f|\hat{h}(\boldsymbol{r})|\Psi_f\rangle$ is

given by

$$\hat{h}_a(\boldsymbol{r}) = \epsilon_{31}|3\rangle\langle 3| - \hbar\chi(\boldsymbol{r})\left(\beta e^{-i\ell\phi}|3\rangle\langle 1| + \alpha e^{i\ell\phi}|3\rangle\langle 2| + h.c.\right) \tag{2}$$

The eigensolutions arising purely from the Hamiltonian for the electronic degree $\hat{h}_a(\boldsymbol{r})|X\rangle = \varepsilon_X|X\rangle$ are given by $|D\rangle$, $|S\rangle$, and $|A\rangle$. The state

$$|D\rangle = \frac{1}{\sqrt{\mathcal{N}}}(\alpha e^{i\ell\phi}|1\rangle - \beta e^{-i\ell\phi}|2\rangle) \tag{3}$$

is known as the *dark* state [20, 21, 22], characterized by a zero eigenvalue $\varepsilon_D = 0$. Here $\mathcal{N} = |\alpha|^2 + |\beta|^2$ is the normalization constant. The two other eigensolutions are given by the symmetric and antisymmetric superposition of the *bright* state $|B\rangle$ and excited state $|3\rangle$,

$$|S\rangle = \frac{1}{\sqrt{2}}(|B\rangle + |3\rangle) \tag{4}$$

$$|A\rangle = \frac{1}{\sqrt{2}}(|B\rangle - |3\rangle) \tag{5}$$

with the eigenvalues $\varepsilon_S = \mathcal{N}$, $\varepsilon_A = -\mathcal{N}$, respectively, where

$$|B\rangle = \frac{1}{\sqrt{\mathcal{N}}}(\beta^* e^{i\ell\phi}|1\rangle + \alpha^* e^{-i\ell\phi}|2\rangle). \tag{6}$$

If the electronic state of an atom is prepared in the dark state $|D\rangle$, the resonant control and probe beams induce the absorption paths $|2\rangle \to |3\rangle$ and $|1\rangle \to |3\rangle$ which interfere destructively. This is also the mechanism behind electromagnetically induced transparency [20, 21, 22]. In such a situation, the transitions to the upper atomic level $|3\rangle$ are suppressed, the atomic level $|3\rangle$ is weakly populated, and it is justified to neglect any losses due to spontaneous emission from the excited state. We shall hereafter assume that the trapped atom is prepared in the dark state.

The total Hamiltonian which accounts for both the electronic and motional dynamics is

$$\hat{H} = \frac{\hat{\boldsymbol{p}}^2}{2M} + \hat{V}(\boldsymbol{r}) + \hat{h}(\boldsymbol{r}) \tag{7}$$

with M being the atomic mass, $\hat{\boldsymbol{p}} = -i\hbar\nabla$ the momentum operator, and

$$\hat{V}(\boldsymbol{r}) = V_1(\boldsymbol{r})|1\rangle\langle 1| + V_2(\boldsymbol{r})|2\rangle\langle 2| + V_3(\boldsymbol{r})|3\rangle\langle 3| \tag{8}$$

is the trapping potential. The entire quantum state including both the atom and field can be written as

$$|\Phi(\boldsymbol{r},t)\rangle = |\Psi_f\rangle \sum_{X=D,S,A} \Psi_X(\boldsymbol{r},t)|X\rangle \tag{9}$$

where $\Psi_X(\boldsymbol{r},t)$ describes the translational motion of the atom in one of the three electronic states. By using this state and the total Hamiltonian (7) we arrive at the equation of motion for the three states $\boldsymbol{\Psi} = (\Psi_D, \Psi_S, \Psi_A)^T$,

$$i\hbar\frac{\partial}{\partial t}\boldsymbol{\Psi} = \hat{H}^{(\text{eff})}\boldsymbol{\Psi} \tag{10}$$

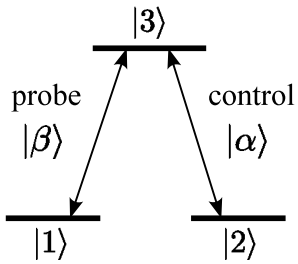

Figure 1. The level scheme. A single atom is irradiated by two lasers: the probe field that couples $|1\rangle$ and $|3\rangle$, with the amplitude β, winding number ℓ_p, frequency ω_p, wavenumber $\boldsymbol{k}_p$, and control field that couples $|2\rangle$ and $|3\rangle$ with the amplitude α, winding number ℓ_c, frequency ω_c, and wavenumber $\boldsymbol{k}_c$. Here we take $\ell = \ell_c = -\ell_p$.

where the effective Hamiltonian is given by

$$\hat{H}^{(\mathrm{eff})} = \frac{1}{2M}(i\hbar\nabla - \boldsymbol{A})^2 + U \tag{11}$$

with

$$\boldsymbol{A}_{X,X'} = -i\hbar\langle X|\nabla X'\rangle, \tag{12}$$

$$U_{X,X'} = \varepsilon_X \delta_{X,X'} + \langle X|\hat{V}|X'\rangle. \tag{13}$$

If the internal dynamics is much faster than the external one we can safely assume the dynamics of the different states to be independent. In other words, the adiabatic approximation is assumed to hold here.

2.2. Dark state and the effective flux tube

In the following we assume that the atom stays in the dark state while moving in space. The total effective Hamiltonian for the center-of-mass motion of the atom in the dark state is given from Eq. (11) as

$$\hat{H}^{(\mathrm{eff})}_{DD} = \frac{1}{2M}(i\hbar\nabla - \boldsymbol{A}_{DD})^2 + V_{\mathrm{eff}} \tag{14}$$

The resulting gauge potential is defined as

$$\boldsymbol{A}_{DD} = -i\hbar\langle D|\nabla D\rangle \boldsymbol{e}_\phi = \frac{\hbar\ell\sigma}{r}\boldsymbol{e}_\phi \tag{15}$$

where

$$\sigma \equiv \frac{|\alpha|^2 - |\beta|^2}{\mathcal{N}} \tag{16}$$

is the mean spin of the two LG laser beams. The effective potential is given by

$$V_{\mathrm{eff}} = U + \varphi, \tag{17}$$

where

$$\varphi = \frac{1}{2M}\sum_{X=S,A} \boldsymbol{A}_{D,X}\boldsymbol{A}_{X,D}. \tag{18}$$

For the dark state, the scalar potential is

$$\varphi = \frac{\hbar^2}{2M}(\langle D|\nabla D\rangle^2 + \langle \nabla D|\nabla D\rangle), \tag{19}$$

and the effective Hamiltonian for the external motion of an atom in the dark state is

$$\hat{H}_{DD}^{(\mathrm{eff})} = \frac{\hbar^2(-\nabla^2 + \langle \nabla D|\nabla D\rangle)}{2M} + \langle D|V(\boldsymbol{r})|D\rangle - \frac{\hbar^2}{M}\langle D|\nabla D\rangle\nabla. \tag{20}$$

Note that with our Hamiltonian (1) and LG beams with the lowest radial quantum number, the dark state depends only on the angle. In this way, the effective trapping potential V_{eff} is composed of the external trapping potential and the geometric scalar potential φ. Drawing these results together the effective Hamiltonian becomes

$$\hat{H}_{DD}^{(\mathrm{eff})} = -\frac{\hbar^2\nabla^2}{2M} + \frac{\hbar^2\ell^2}{2Mr^2} + V(\boldsymbol{r}) - i\ell\sigma\frac{\hbar^2}{Mr^2}\frac{\partial}{\partial\phi}. \tag{21}$$

For simplicity in notation we hereafter omit the subscript D for the dark state unless otherwise stated.

The angular-momentum operator for the dark state atom is given by

$$\hat{L}_z = |D\rangle\langle D|\left(-i\hbar\frac{\partial}{\partial\phi}\right)|D\rangle\langle D|, \tag{22}$$

which has an additional term that comes from the dark-state spatial variation,

$$\langle D|\left(-i\hbar\frac{\partial}{\partial\phi}\right)|D\rangle = -i\hbar\frac{\partial}{\partial\phi} + rA_\phi, \tag{23}$$

where $A_\phi = \hbar\ell\sigma/r$ is the ϕ component of the gauge potential Eq. (15). If the mean spin of two lasers σ is non-integer, the orbital angular momentum of the motional state is no longer quantized in the integer units of $\hbar$. Finally, the effective magnetic flux induced by the effective gauge potential is given by

$$\Phi_{\mathrm{mf}} = 2\pi\hbar\sigma\ell, \tag{24}$$

The effective gauge potential due to the applied LG fields therefore acts as a flux tube of strength Φ_{mf}.

2.2.1. Ring geometry First we consider the case that the atom is tightly trapped circumferentially on a ring of radius R by an external annular potential, which greatly simplifies the analysis [16, 17]. The effective Hamiltonian at a fixed radius $r = R$ is

$$\hat{H}^{(\mathrm{eff})} = \frac{\hbar^2}{2I}\left(-\frac{\partial^2}{\partial\phi^2} + \ell^2 - 2i\ell\sigma\frac{\partial}{\partial\phi}\right) \tag{25}$$

where we have defined the rotational inertia $I = MR^2$. The solutions of the eigenproblem $\hat{H}^{(\mathrm{eff})}\Psi = E\Psi$ for the atomic motional state with the electronic state being the dark state are specified only by angular-momentum quantum number m,

$$E_m = \frac{\hbar^2}{2I}(\ell^2 + m^2 + 2\sigma\ell m) \tag{26}$$

$$\Psi_m(\phi) = \frac{1}{\sqrt{2\pi}}e^{im\phi} \tag{27}$$

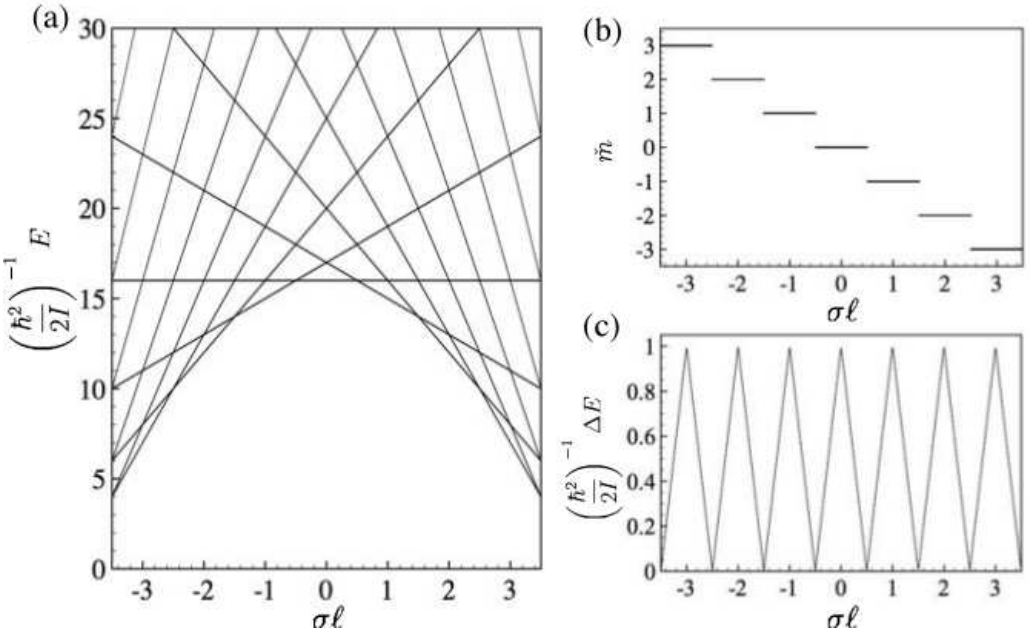

Figure 2. (a) Energy eigenvalues $E_m/(\hbar^2/2I)$, (b) ground-state angular momentum $\check{m}$, and (c) the lowest excitation energy $\Delta E/(\hbar^2/2I)$, as a function of the mean spin, for $\ell = 4$.

where $m \in \{0, \pm 1, \pm 2, \ldots\}$. Generally the energy E_m for a given value of $\sigma\ell$, and E_{-m} for the value $-\sigma\ell$ are degenerate. The quantum number for the ground state $\check{m}$ is given by

$$\check{m} = -\lfloor \sigma\ell + 1/2 \rfloor, \tag{28}$$

where $\lfloor s \rfloor$ denotes the floor function applied to the argument s. We note that we have $\mathrm{sgn}(\sigma\ell\check{m}) < 0$: this fact will be important in the next Section in evaluating the energy associated with the superposition. The energy eigenvalues E_m, and the ground-state angular momentum $\check{m}$ for $\ell = 4$ are plotted as a function of $\sigma\ell$ in Fig. 2 (a), (b), respectively.

Figure 2 (c) plots the energy separation between the ground and the first excited states, $\Delta E \equiv E_{\check{m}\pm 1} - E_{\check{m}} = (\hbar^2/2I)\,[\pm 2(\check{m} + \sigma\ell) - 1]$. This energy gap becomes zero at half-integral values of the mean spin σ, and the ground-state angular momentum $\check{m}$ changes at these points. On the other hand, ΔE takes local maxima at integral values of $\sigma\ell$. Because of the restriction of the atomic motion to the ring, the excitation energy as a function of $\sigma\ell$ is independent of ℓ.

2.2.2. Harmonic trapping potential When the atom is trapped in a harmonic trap $V(r) = M\Omega^2 r^2/2$, the eigenproblem for the motional state of the dark-state atom is also analytically solvable [15]. With the use of the zero-point oscillator length $r_0 = \sqrt{\hbar/(2M\Omega)}$ as the length unit, the Hamiltonian is

$$\hat{H}^{(\mathrm{eff})} = \hbar\Omega \left[-\nabla^2 + \frac{r^2}{4} + \frac{1}{r^2}\left(\ell^2 - 2i\ell\sigma \frac{\partial}{\partial\phi} \right) \right], \tag{29}$$

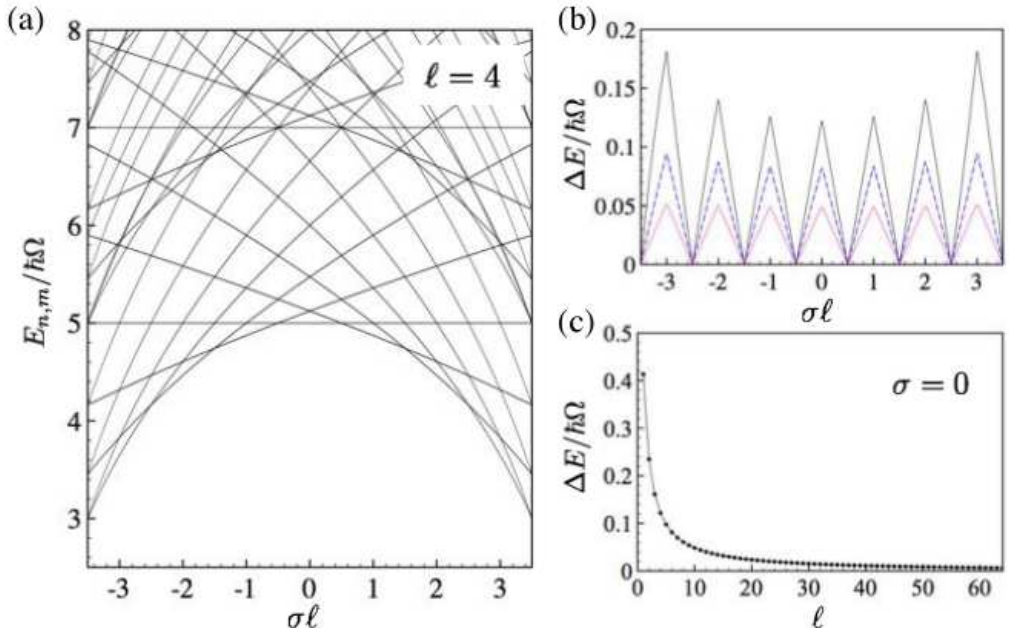

Figure 3. (a) Energy eigenvalues $E_{n,m}/\hbar\Omega$ as a function of $\sigma\ell$. Here we fixed the winding number $\ell = 4$. (b) The lowest excitation energy for $\ell = 4$ (line), 6 (dashed), and 10 (dotted). (c) The lowest excitation energy at $\sigma = 0$ as a function of ℓ.

and its eigenvalues and eigenstates are given by

$$E_{n,m} = \hbar\Omega(2n + \mu_m + 1) \tag{30}$$

$$\Psi_{n,m}(\boldsymbol{r}) = \frac{1}{\sqrt{2\pi}} e^{im\phi} f_{n,m}(r) \tag{31}$$

where $n \in \{0, 1, \ldots\}$ and $m \in \{0, \pm 1, \pm 2, \ldots\}$. The radial dependence of the eigenstate is obtained as

$$f_{n,m}(r) = C_{n,m} \left(\frac{r^2}{2}\right)^{\mu_m/2} e^{-r^2/4} \mathcal{L}_n^{\mu_m}\left(\frac{r^2}{2}\right), \tag{32}$$

where $C_{n,m} = \sqrt{n!/\Gamma(n + \mu_m + 1)}$ with $\Gamma(x)$ being the Gamma function. The function $\mathcal{L}_n^{\alpha}(x)$ is the generalized Laguerre polynomial, parametrized with

$$\mu_m = \sqrt{\ell^2 + m^2 + 2\sigma\ell m}. \tag{33}$$

Just like the case of the ring geometry, the eigenvalues $E_{n,m}$ for a given value of $\sigma\ell$ is degenerate with $E_{n,-m}$ for the value $-\sigma\ell$. The quantum numbers $(\check{n}, \check{m})$ of ground state are given by

$$\check{n} = 0, \quad \check{m} = -\lfloor \sigma\ell + 1/2 \rfloor, \tag{34}$$

and therefore we again have $\mathrm{sgn}(\sigma\ell\check{m}) < 0$ for the ground state. The energy eigenvalues $E_{n,m}$ for various n with $\ell = 4$ are plotted as a function of $\sigma\ell$ in Fig. 3 (a).

Figure 3 (b) plots the energy separation ΔE between the ground and the first excited states. This energy gap similarly becomes zero at half-integral values of the mean spin σ and takes local maxima at integral value of σ. In contrast to the ring case,

for a fixed value of ℓ while changing the mean spin σ, the magnitudes of ΔE at different integral values of $|\sigma\ell|$ are different values as $\Delta E(\sigma\ell = 0) \lesssim \Delta E(|\sigma\ell| = 1) \lesssim \Delta E(|\sigma\ell| = 2) \lesssim \cdots$. When we inspect the energy gap as a function of ℓ for a fixed value of mean spin (say, $\sigma = 0$), ΔE is a monotonically decreasing function with respect to ℓ as shown in Fig. 3 (c).

3. Superposition in atomic quantum rings

The goal of this section is to demonstrate that by making the control field a quantum superposition of coherent states the trapped atom can be made to experience a combination of flux tubes with opposite sign of flux [15, 16, 17]. Furthermore we show that the ground state for both harmonic trapping and a ring geometry is a superposition of rotating atomic states in the individual flux tubes.

In the following we consider a control field that is described by a quantum superposition of coherent states $|\alpha_+\rangle$ and $|\alpha_-\rangle$ whereas the probe field is described by the single coherent state $|\beta\rangle$ as in the previous section. More specifically we choose $\alpha_\pm$ as real and β as complex where a relative phase is included in β. The total field state is then written as

$$|\Psi_f\rangle \propto (|\alpha_+\rangle + e^{i\theta}|\alpha_-\rangle)|\beta\rangle, \tag{35}$$

where θ is the relative phase between the two coherent state components in the control field.

Let us first examine the nature of the atom-field state corresponding to each coherent state component of the quantum superposition separately. Then for the two components associated with the coherent states $|\alpha_\pm\rangle$, the total quantum state including field, and the atomic motional and internal states may be written as

$$|\Phi_\pm(\boldsymbol{r})\rangle = \Psi_\pm(\boldsymbol{r})|D_\pm(\phi)\rangle|\alpha_\pm\rangle|\beta\rangle, \tag{36}$$

where the dark state in each component is respectively given from the discussion in the previous section:

$$|D_\pm(\phi)\rangle = \frac{1}{\sqrt{\mathcal{N}_\pm}}\left(\alpha_\pm e^{i\ell\phi}|1\rangle - \beta e^{-i\ell\phi}|2\rangle\right), \tag{37}$$

with $\mathcal{N}_\pm = \alpha_\pm^2 + |\beta|^2$ a normalization constant. We also define the mean spin for each component as

$$\sigma_\pm \equiv \frac{\alpha_\pm^2 - |\beta|^2}{\alpha_\pm^2 + |\beta|^2}. \tag{38}$$

We are now in a position to describe our scheme more specifically: In particular, we want to choose the amplitudes $\alpha_\pm$ such that the two coherent-state components correspond to flux tubes of opposite sign which requires that the mean spins of the two components are opposite in sign $\sigma_+ = -\sigma_- = \sigma$. Using Eq. (38) we find that the coherent-state amplitudes have to obey either of the following two conditions

$$\text{(i)} \quad |\beta|^2 = \alpha_+\alpha_- \tag{39}$$

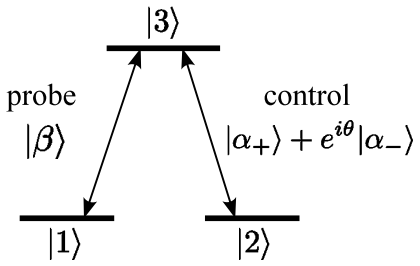

Figure 4. Level scheme to generate flux tubes with opposite sign. The control field is a superposition of coherent states $|\alpha_+\rangle$ and $|\alpha_-\rangle$.

or

$$\text{(ii)} \quad |\beta|^2 = -\alpha_+\alpha_-. \tag{40}$$

When either of these two conditions is satisfied, the two components of the coherent state correspond to situations in which the trapped particle will experience flux tubes with fluxes $\Phi_{\rm mf} = \pm 2\pi\hbar|\sigma\ell|$ of equal magnitude but opposite sign. However, from the perspective of the fragility of optical coherent state superpositions against interactions with their enviroment case (i) above is preferable. This follows since the optical coherent state superpositions decay as $\exp(-|\alpha_+ - \alpha_-|^2\gamma t/2)$ [18], with γ a constant dependent on the specific dissipation mechanism, so that having $\alpha_\pm$ of the same sign will yield a state less fragile against enviromental factors. Glancy and Macedo de Vasconcelos [19] have reviewed methods for producing optical coherent state superpositions. For our present purposes we require a superposition of coherent states that are macroscopically distinguishable but not necessarily macroscopically separated, with the mean photon numbers $|\alpha_\pm|^2$ separated by only a few quanta. The feasibility of creating such optical coherent state superpositions was already alluded to in the seminal work of Ref. [23].

We next turn the normalized quantum state for the combined atom-field system including both components of the coherent state

$$|\Phi(\boldsymbol{r},t)\rangle = \frac{|\Phi_+\rangle + e^{i\theta}|\Phi_-\rangle}{\sqrt{2[1+|\langle\Phi_+|\Phi_-\rangle|\cos(\theta+\psi)]}}, \tag{41}$$

where $\langle\Phi_+|\Phi_-\rangle \equiv |\langle\Phi_+|\Phi_-\rangle|e^{i\psi}$. We note that the relative phase between the field coherent state components also appears in the atom-field quantum state. Consistency demands that the normalized state vector (41) obeys the Schrödinger equation

$$i\hbar\frac{\partial}{\partial t}|\Phi(\boldsymbol{r},t)\rangle = \hat{H}|\Phi(\boldsymbol{r},t)\rangle \tag{42}$$

where $\hat{H}$ is given by Eq. (7).

Our next goal is to derive equations of motion for the atomic motional wavefunctions $\Psi_\pm$ corresponding to the two coherent-state components. However, this is complicated by the fact that $|\Phi_\pm\rangle$ need not be orthogonal which originates from the fact that the coherent states $|\alpha_\pm\rangle$ are not orthogonal, and this means that cross terms between the components must be retained. In particular, we need the matrix elements of the

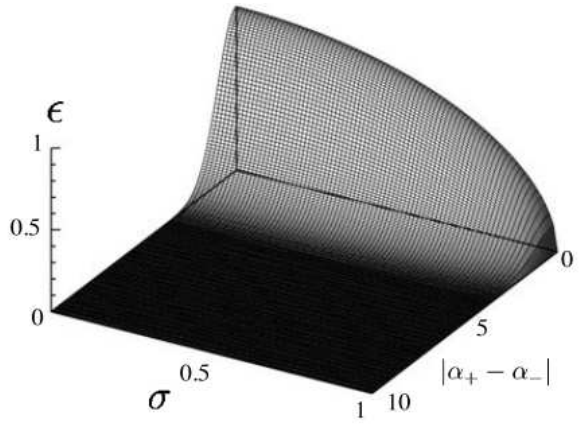

Figure 5. Parameter ϵ as functions of $|\alpha_+ - \alpha_-|$ and σ.

Hamiltonian with respect to the dark states $|D_\pm\rangle$, and we quote these results here:

$$\langle D_\pm|H|D_\pm\rangle = \hat{K} - \frac{\hbar^2}{M}\langle D_\pm|\nabla D_\pm\rangle\nabla \tag{43}$$

$$\langle D_\pm|H|D_\mp\rangle = \hat{K}\langle D_\pm|D_\mp\rangle - \frac{\hbar^2}{M}\langle D_\pm|\nabla D_\mp\rangle\nabla \tag{44}$$

where

$$\hat{K} \equiv \frac{\hbar^2}{2M}\left(-\nabla^2 + \frac{M^2\Omega^2 r^2}{\hbar^2} + \frac{\ell^2}{r^2}\right) \tag{45}$$

for the harmonic potential, and

$$\hat{K} \equiv \frac{\hbar^2}{2I}\left(-\frac{\partial^2}{\partial\phi^2} + \ell^2\right) \tag{46}$$

for the ring trap of radius R. The cross terms between different dark states are given by

$$\langle D_\pm|D_\mp\rangle = \frac{\alpha_+\alpha_- + |\beta|^2}{\sqrt{\mathcal{N}_+\mathcal{N}_-}}, \tag{47}$$

$$\langle D_\pm|\nabla D_\mp\rangle = \frac{i\ell(\alpha_+\alpha_- - |\beta|^2)}{r\sqrt{\mathcal{N}_+\mathcal{N}_-}}. \tag{48}$$

The above results will be used to obtain the equations of motion for the wavefunctions $\Psi_\pm$ of the two coherent-state components by substituting the state vector in Eq. (41) into Eq. (42), and projecting onto the two (non-orthogonal) components. In the following we deal with the two conditions set out in Eqs. (39) and (40) separately.

3.1. Case (i) $|\beta|^2 = \alpha_+\alpha_-$

For this case the cross terms between the dark states reduce to

$$\langle D_\pm|D_\mp\rangle = \sqrt{1-\sigma^2}, \quad \langle D_\pm|\nabla D_\mp\rangle = 0. \tag{49}$$

Then projecting from the left onto the Schrödinger equation (42) using $\langle D_\pm|\langle\alpha_\pm|\langle\beta|$ generates the following set of equations for the wavefunctions $\Psi_\pm(\boldsymbol{r})$ for the atomic external degree of freedom

$$i\hbar\frac{\partial}{\partial t}[\Psi_+ + \epsilon e^{i\theta}\Psi_-] = \left(\hat{K} - \frac{\hbar^2}{M}\langle D_+|\nabla D_+\rangle\nabla\right)\Psi_+ + \epsilon e^{i\theta}\hat{K}\Psi_- \tag{50}$$

$$i\hbar\frac{\partial}{\partial t}[\epsilon e^{-i\theta}\Psi_+ + \Psi_-] = \epsilon e^{-i\theta}\hat{K}\Psi_+ + \left(\hat{K} - \frac{\hbar^2}{M}\langle D_-|\nabla D_-\rangle\nabla\right)\Psi_-, \tag{51}$$

where the following real parameter characterizes the non-orthogonality of two components

$$\epsilon = \langle\alpha_+|\alpha_-\rangle\sqrt{1-\sigma^2} = e^{-|\alpha_+ - \alpha_-|^2}\sqrt{1-\sigma^2}. \tag{52}$$

Figure 5 shows the dependence of ϵ on σ and $|\alpha_+ - \alpha_-|$, and shows that we may control the size of ϵ by controlling the difference between the coherent state amplitudes $\alpha_\pm$. In keeping with case (i) reflected in Eq. (39), if $\alpha_\pm$ have the same sign and differ in magnitude squared by a few quanta we may control $0 \leq \epsilon \leq 1$ for a given σ. Typically we want ϵ small, say 1/10, but not too small.

3.1.1. Ring geometry First we consider the ring geometry as this allows us to illustrate the basic ideas involved with the least complexity. For the ring case the atom is constrained to move on a circle of radius R with position parameterized by the azimuthal angle ϕ. In order to evaluate the energy of superposition state, we use the ansatz for the ground-state wavefunctions

$$\Psi_\pm(\phi) \propto (\xi_\pm e^{i\check{m}\phi} + \zeta_\pm e^{-i\check{m}\phi})e^{-iEt/\hbar}, \tag{53}$$

where $\xi_\pm, \zeta_\pm$ are c-numbers. This ansatz is motivated by the fact that in the approximation that the coherent-state components are treated as orthogonal ($\epsilon \to 0$), the solutions of Eqs. (50) and (51) should coincide with those given in subsection 2.2.1. In particular, the solutions $\Psi_+ \propto e^{i\check{m}\phi}$ and $\Psi_- \propto e^{-i\check{m}\phi}$ correspond to the rotating ground-state eigenfunctions of the Hamiltonian (25) for $+\sigma\ell$ and $-\sigma\ell$. Furthermore, the energies of the rotating eigenfunctions $\Psi_\pm$ are degenerate,

$$E_0 = \frac{\hbar^2}{2I}(\ell^2 + \check{m}^2 + 2\sigma\ell\check{m}). \tag{54}$$

Figure 2 illustrates the degeneracy of the ground states for values $\pm\sigma\ell$ for the case with no cross-coupling $\epsilon = 0$. However, in the presence of cross coupling the angular momentum states with $\pm\check{m}$ become inter-mixed, hence the form of the ansatz (53). The key question to be addressed is whether cross-coupling with $\epsilon \neq 0$ can lower the ground-state energy of the system. If so then the state vector in Eq. (41), which represents a superposition of the atom trapped simultaneously on the two different flux tubes, will have an energy lower than a simple mixture state of the atom trapped on one or other of the two flux tubes that has energy E_0. Furthermore the energetically favored ground state will have the form of a quantum superposition of the atom in the counter-rotating angular momentum states $\pm\hbar\check{m}$.

To determine the ground state energy in the presence of cross-coupling, we substitute (53) into Eqs. (50) and (51), and use the orthogonality of the spatial modes $e^{\pm i\check{m}\phi}$, to obtain equations for $\xi_\pm$ and $\zeta_\pm$ as

$$\frac{\hbar^2}{2I}\begin{bmatrix} \ell^2+\check{m}^2+2\sigma\ell\check{m} & e^{i\theta}\epsilon(\ell^2+\check{m}^2) \\ e^{-i\theta}\epsilon(\ell^2+\check{m}^2) & \ell^2+\check{m}^2-2\sigma\ell\check{m} \end{bmatrix}\begin{bmatrix} \xi_+ \\ \xi_- \end{bmatrix} = E\boldsymbol{A}\begin{bmatrix} \xi_+ \\ \xi_- \end{bmatrix} \tag{55}$$

$$\frac{\hbar^2}{2I}\begin{bmatrix} \ell^2+\check{m}^2-2\sigma\ell\check{m} & e^{i\theta}\epsilon(\ell^2+\check{m}^2) \\ e^{-i\theta}\epsilon(\ell^2+\check{m}^2) & \ell^2+\check{m}^2+2\sigma\ell\check{m} \end{bmatrix}\begin{bmatrix} \zeta_+ \\ \zeta_- \end{bmatrix} = E\boldsymbol{A}\begin{bmatrix} \zeta_+ \\ \zeta_- \end{bmatrix} \tag{56}$$

where

$$\boldsymbol{A} = \begin{bmatrix} 1 & \epsilon e^{i\theta} \\ \epsilon e^{-i\theta} & 1 \end{bmatrix}. \tag{57}$$

These equations have common eigenvalues $E = \{E_+, E_-\}$,

$$\left(\frac{\hbar^2}{2I}\right)^{-1} E_\pm = \ell^2+\check{m}^2 \pm \frac{2\sigma\ell\check{m}}{\sqrt{1-\epsilon^2}}. \tag{58}$$

Among these two eigenvalues, only E_+ is relevant here as it coincides with the degenerate ground-state energy E_0 in the limit $\epsilon \to 0$. The energy difference associated with the superposition $\delta E \equiv E_+ - E_0$ is therefore given by

$$\left(\frac{\hbar^2}{2I}\right)^{-1}\delta E = 2\sigma\ell\check{m}\left(\frac{1}{\sqrt{1-\epsilon^2}}-1\right) \tag{59}$$

which is *negative* since $\mathrm{sgn}(\sigma\ell\check{m}) < 0$ for the ground state, see the discussion surrounding Eq. (28). The superposition state thus has a lower energy than that of the mixed states of two coherent state components. For small ϵ this reduction in energy is written as $(\hbar^2/2I)^{-1}\delta E \simeq -|\sigma\ell\check{m}|\epsilon^2$, which is of the order of ϵ^2.

It is preferable to have a larger reduction in energy $|\delta E|$ in terms of robustness. On the other hand, $|\delta E|$ should not be larger than the lowest excitation energy ΔE from the ground state in the absence of superposition; otherwise the ansatz (53) is no longer valid. Therefore, from the examination of the eigenvalue structure, we employ an integral value of $\sigma\ell$, where the energy gap takes maximum value $\Delta E = \hbar^2/(2I)$. Figure 6 plots the magnitude of the energy gain $|\delta E|$ in the region where $|\delta E| < \Delta E$. The corresponding parameter ϵ is also plotted. When $|\delta E|/(\hbar^2/2I)$ is not too small (~ 0) and nor too large (~ 1); e.g., at $|\alpha_+ - \alpha_-| \simeq 3$ the superposition is feasible.

The eigenvectors $\{\xi_\pm, \zeta_\pm\}$, corresponding to the eigenvalue E_+, give the admixture of the distinct rotational states with winding numbers $\pm\check{m}$ in the ground state superposition. These eigenvectors are obtained as

$${}^t[\xi_+, \xi_-] \propto {}^t[-\epsilon e^{i\theta}, 1-\sqrt{1-\epsilon^2}], \quad {}^t[\zeta_+, \zeta_-] \propto {}^t[-\epsilon e^{i\theta}, 1+\sqrt{1-\epsilon^2}]. \tag{60}$$

Thus for $\epsilon \ll 1$ we find

$$\left|\frac{\xi_-}{\xi_+}\right|^2 = \left|\frac{\zeta_+}{\zeta_-}\right|^2 = \frac{\epsilon^2}{4} \ll 1, \tag{61}$$

which means that there is little mixing between the rotational states, and we have a superposition of counter-rotating states to a high degree.

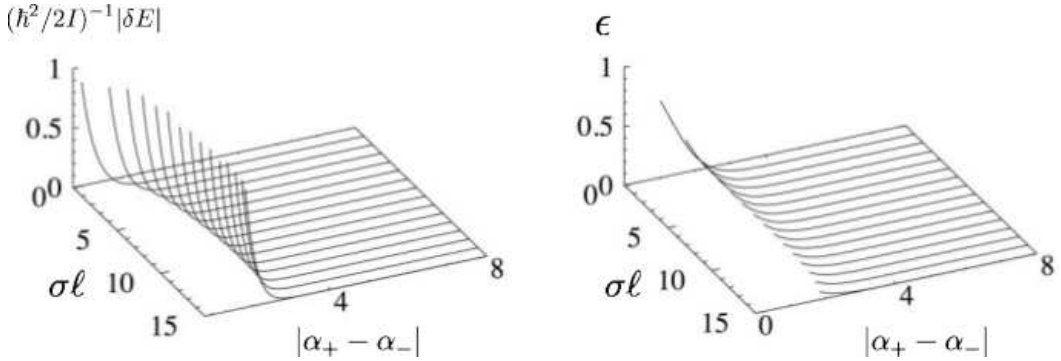

Figure 6. Magnitude of energy reduction as functions of the integer values of $\sigma\ell$ and $|\alpha_+ - \alpha_-|$ for $\ell = 16$.

3.1.2. Harmonic trapping We now repeat the same procedure for the case of harmonic trapping which modifies the details but not the concept of the superposition state. We employ the similar ansatz for wavefunctions,

$$\Psi_\pm(r,\phi) \propto [\xi_\pm e^{i\check{m}\phi} + \zeta_\pm e^{-i\check{m}\phi}] R_{\check{m}}(r) e^{-iEt/\hbar} \tag{62}$$

where

$$R_{\check{m}}(r) \equiv f_{0\check{m}}(r) = \sqrt{\frac{2M\Omega}{\hbar\Gamma(\mu_{\check{m}}+1)}} \left(\frac{M\Omega r^2}{\hbar}\right)^{\mu_{\check{m}}/2} e^{-\frac{M\Omega}{2\hbar}r^2} \tag{63}$$

is the radial eigenfunction of Eq. (32) for the ground-state quantum numbers $n = 0, m = \check{m}$. Similar calculation as in the ring-geometry case yeilds equations for $\xi_\pm, \zeta_\pm$ for the harmonic-trapping case as

$$\hbar\Omega \begin{bmatrix} \eta + \sigma\ell\check{m}/\mu_{\check{m}} & e^{i\theta}\epsilon\eta \\ e^{-i\theta}\epsilon\eta & \eta - \sigma\ell\check{m}/\mu_{\check{m}} \end{bmatrix} \begin{bmatrix} \xi_+ \\ \xi_- \end{bmatrix} = E\boldsymbol{A} \begin{bmatrix} \xi_+ \\ \xi_- \end{bmatrix} \tag{64}$$

$$\hbar\Omega \begin{bmatrix} \eta - \sigma\ell\check{m}/\mu_{\check{m}} & e^{i\theta}\epsilon\eta \\ e^{-i\theta}\epsilon\eta & \eta + \sigma\ell\check{m}/\mu_{\check{m}} \end{bmatrix} \begin{bmatrix} \zeta_+ \\ \zeta_- \end{bmatrix} = E\boldsymbol{A} \begin{bmatrix} \zeta_+ \\ \zeta_- \end{bmatrix} \tag{65}$$

where $\boldsymbol{A}$ is given by Eq. (57), and $\eta \equiv \mu_{\check{m}} + 1 - \sigma\ell\check{m}/\mu_{\check{m}}$. The common eigenvalues are

$$\frac{E_\pm}{\hbar\Omega} = \eta \pm \frac{\sigma\ell\check{m}}{\mu_{\check{m}}\sqrt{1-\epsilon^2}} \tag{66}$$

and again E_+ is relevant, since in the limit $\epsilon \to 0$ it coincides with the degenerate ground-state energy in the harmonic trapping potential, $E_0 = \hbar\Omega(\mu_{\check{m}} + 1)$. The energy difference between the superposition and mixture is

$$\frac{\delta E}{\hbar\Omega} = \frac{\sigma\ell\check{m}}{\mu_{\check{m}}} \left(\frac{1}{\sqrt{1-\epsilon^2}} - 1\right), \tag{67}$$

which is negative by virtue of the fact that $\mathrm{sgn}(\sigma\ell\check{m}) < 0$, i.e., the superposition has a lower energy than the mixture. For small ϵ, this reduction in energy is written as $\delta E/\hbar\Omega \simeq -|\sigma\ell\check{m}|\epsilon^2/(2\mu_{\check{m}})$, which is again of the order of ϵ^2.

In the harmonic trap, the largest energy gap between $E_{\check{m}}$ and $E_{\check{m}\pm1}$ is possible also at the integral values of $\ell\sigma$. However, this energy gap gets smaller for larger value of

orbital angular momentum of LG beam, ℓ. Figure plots the region where $|\delta E|$ is smaller than energy gap in Fig. 3.

The eigenvectors corresponding to the eigenvalue E_+ are found to be equivalent to the case of the ring trap Eq. (60). Thus, we have a superposition of counter-rotating states in the case of the harmonic trapping, too.

3.2. Case (ii) $|\beta|^2 = -\alpha_+\alpha_-$

In this case the cross terms of dark states reduce to

$$\langle D_\pm|D_\mp\rangle = 0, \quad \langle D_\pm|\nabla D_\mp\rangle = -\frac{i\ell}{r}\sqrt{1-\sigma^2}. \tag{68}$$

Following the same procedure as in the case (i), the Schrödinger equation is obtained as

$$i\hbar\frac{\partial}{\partial t}\Psi_+(\boldsymbol{r}) = \left(\hat{K} - \frac{\hbar^2}{M}\langle D_+|\nabla D_+\rangle\nabla\right)\Psi_+(\boldsymbol{r}) + \epsilon e^{i\theta}\frac{i\hbar^2\ell}{Mr}\nabla\Psi_-(\boldsymbol{r}) \tag{69}$$

$$i\hbar\frac{\partial}{\partial t}\Psi_-(\boldsymbol{r}) = \epsilon e^{-i\theta}\frac{i\hbar^2\ell}{Mr}\nabla\Psi_+(\boldsymbol{r}) + \left(\hat{K} - \frac{\hbar^2}{M}\langle D_-|\nabla D_-\rangle\nabla\right)\Psi_-(\boldsymbol{r}) \tag{70}$$

where ϵ is defined by Eq. (52). We again study the cases of ring potential, and harmonic potential, respectively, and show only the results here without commentary.

3.2.1. Ring potential With the use of the same ansatz (53), we obtain the difference in the energy of superposition and that of mixture $\delta E \equiv E_+ - E_0$ as

$$\left(\frac{\hbar^2}{2I}\right)^{-1}\delta E = 2\ell\check{m}(\sqrt{\epsilon^2+\sigma^2} - \sigma) \tag{71}$$

where we again employed the solution that coincides with E_0 in the limit $\epsilon \to 0$. For small ϵ, this is expanded as

$$\left(\frac{\hbar^2}{2I}\right)^{-1}\delta E \simeq \frac{\ell\check{m}\epsilon^2}{\sigma} \tag{72}$$

which is again negative meaning that the superposition state is energetically favored.

For the integer values of $\sigma\ell$, the condition $|\delta E| < \Delta E$ turned out to be identical to the case (i).

Eigenvectors for the ground state E_+ are

$${}^t[\xi_+, \xi_-] = {}^t[\epsilon e^{i\theta}, \sigma - \sqrt{\epsilon^2+\sigma^2}], \quad {}^t[\zeta_+, \zeta_-] = {}^t[\epsilon e^{i\theta}, \sigma + \sqrt{\epsilon^2+\sigma^2}], \tag{73}$$

and for $\epsilon \ll 1$ we have

$$\left|\frac{\xi_-}{\xi_+}\right|^2 = \left|\frac{\zeta_+}{\zeta_-}\right|^2 = \frac{\epsilon^2}{4\sigma^2} \ll 1. \tag{74}$$

This result again means that there is little mixing between the rotational states, and we have a superposition of counter-rotating states to a high degree.

3.2.2. Harmonic potential The ansatz (62) leads to the energy difference,

$$\frac{\delta E}{\hbar\Omega} = \frac{\ell\check{m}}{\mu_{\check{m}}}(\sqrt{\epsilon^2+\sigma^2}-\sigma). \tag{75}$$

and the corresponding eigenvectors are given by Eq (73). For $\epsilon \ll 1$,

$$\frac{\delta E}{\hbar\Omega} = \frac{\ell\check{m}}{2\sigma\mu_{\check{m}}}\epsilon^2. \tag{76}$$

The energy associated with the superposition and the mixing rate of the rotational states are the order of ϵ^2.

4. Conclusion

In summary, we have introduced the idea of using quantized light fields for the creation of artificial gauge fields and shown that it can yield superpositions in atomic quantum rings. The underlying concept is that by using optical coherent state superpositions one can expose an atom simultaneously to a combination of artificial gauge fields, or in our specific example to a combination of flux tubes. For the atomic quantum ring this was shown to lead to a ground state that was a superposition of counter-rotating atomic states.

It should be noted that a superposition of counter-rotating atomic states can also be created using synthetic spin-orbit coupling [4, 10, 16]. The gauge potential stems in this case from classical light fields and is also static, where each component of the resulting atomic pseudo-spin can experience opposite constant magnetic fields. Artificial gauge potentials formed using quantum mechanical applied light fields, with the possibility of exposing the atom simultaneously to a superposition of two or more artificial gauge potentials, offers some intriguing new concepts. Not only does it provide a route towards mesoscopic superposition states of quantum gases, but it also allows for creation of entanglement between emerging gauge fields and motional degrees of freedom in the quantum gas. It may also provide a route to construct a back-action between the gauge field and the atomic center of mass state by relying on strong coupling between the constituents, and by doing so simulate a dynamical gauge theory.

It is certainly tempting to extend these ideas in several ways including inclusion of many-body effects, treatment of more general quantized light fields, coupling between the light and matter-wave fields in an optical cavity, and the application to more general geometries such as atomic motion in a combination of gauge fields of induced optical lattices.

P.Ö. acknowledges support from the UK EPSRC, and R.K. acknowledges support by Grant-in-Aid for Scientific Research from MEXT (No. 23104712) Japan.

[1] For a recent review see J. Dalibard, F. Gerbier, J. Juzeliūnas, and P. Öhberg, Rev. Mod. Phys. **83**, 1523 (2011).
[2] Y. Lin, R. L. Compton, A. R. Perry, W. D. Phillips, J. V. Porto, and I. Spielman, Phys. Rev. Lett. **102**, 130401 (2009).
[3] Y. J.l Lin, R. L. Compton, K. Jimenez-Garcia, J. V. Porto, and I. B. Spielman, Nature **462**, 628 (2009).
[4] Y. Lin, K. Jimenez-Garcia, and I. Spielman, Nature **471**, 83 (2011).
[5] M. Aidelsburger, M. Atala, S. Nascimbène, S. Trotzky, Y.-A. Chen, and I. Bloch, Phys. Rev. Lett. **107**, 255301 (2011).
[6] K. Osterloh, M. Baig, L. Santos, P. Zoller, and M. Lewenstein, Phys. Rev. Lett. **95**, 010403 (2005).
[7] J. Ruseckas, G. Juzeliūnas, P. Öhberg, and M. Fleischhauer, Phys. Rev. Lett. **95**, 010404 (2005).
[8] M. Burrello and A. Trombettoni, Phys. Rev. Lett. **105**, 125304 (2010).
[9] D. Jaksch and P. Zoller, New Journal of Physics **5**, 56 (2003).
[10] A. Jacob, P. Öhberg, G. Juzeliūnas, L. Santos, Appl. Phys. B **89**, 439 (2007).
[11] M. Merkl, A. Jacob, F. E. Zimmer, P. Öhberg, and L. Santos, Phys. Rev. Lett. **104**, 073603 (2010).
[12] Z. Lan, A. Celi. W. Lu, P. Öhberg, and M. Lewenstein, Phys. Rev. Lett. **107**, 253001 (2011).
[13] L. Mazza, A. Bermudez, N. Goldman, M. A. Martin-Delgado, and M. Lewenstein, New Journal of Physics **14**, 015007 (2012).
[14] G. Juzeliunas, J. Ruseckas, and P. Öhberg, J. Phys. B **38**, 4171 (2005).
[15] J.-J. Song, B.A. Foreman, X.-J. Liu, and C.H. Ou, Eur. Phys. Lett. **84**, 20012 (2008).
[16] J.-J. Song and .A. Foreman, Phys. Rev. A **80**, 033602 (2009).
[17] P. Öhberg, J. Opt. **13**, 1 (2011).
[18] G. J. Milburn and D. F. Walls, *Quantum optics* (Springer, Berlin, 1994), Chap. 16.
[19] For a review of optical coherent state superpositions see, for exmaple, S. Glancy and H. Macedo de Vasconcelos, J. Opt. Soc. Am. B **25**, 712 (2008).
[20] E. Arimondo, Progr. Opt. **35**, 259 (1996).
[21] S.E. Harris, Phys. Today **50**, 36 (1997).
[22] M.D. Lukin, Rev. Mod. Phys. **75**, 457 (2003).
[23] S. Song, and C. M. Caves, and B. Yurke, Phys. Rev. A **41**, 5261 (1990).